Renewable Energy 74 (2015) 326–336

Contents lists available at ScienceDirect

Renewable Energy

journal homepage: www.elsevier.com/locate/renene

freepapers.ir FREE papers

Energy dispatching based on predictive controller of an off-grid wind turbine/photovoltaic/hydrogen/battery hybrid system

Juan P. Torreglosa [a, c], Pablo García [b], Luis M. Fernández [b], Francisco Jurado [a, *]

[a] INYTE Research Group (PAIDI-TEP-152), Department of Electrical Engineering, EPS Linares, University of Jaén, C/Alfonso X, n° 28, 23700 Linares, Jaén, Spain
[b] TESYR Research Group (PAIDI-TEP-023), Department of Electrical Engineering, EPS Algeciras, University of Cádiz, Avda. Ramón Puyol, s/n, 11202 Algeciras, Cádiz, Spain
[c] Universidad Autónoma de Chile, Avenida Alemania, 01090 Temuco, Chile

ARTICLE INFO

Article history:
Received 27 December 2013
Accepted 4 August 2014
Available online

Keywords:
Energy dispatching
Hydrogen system
Off-grid system
Predictive control
Renewable energy

ABSTRACT

This paper presents a novel energy dispatching based on Model Predictive Control (MPC) for off-grid photovoltaic (PV)/wind turbine/hydrogen/battery hybrid systems. The renewable energy sources supply energy to the hybrid system and the battery and hydrogen system are used as energy storage devices. The denominated "hydrogen system" is composed of fuel cell, electrolyzer and hydrogen storage tank. The MPC generates the reference powers of the fuel cell and electrolyzer to satisfy different objectives: to track the load power demand and to keep the charge levels of the energy storage devices between their target margins. The modeling of the hybrid system was developed in MATLAB-Simulink, taking into account datasheets of commercially available components. To show the proper operation of the proposed energy dispatching, a simpler strategy based on state control was presented in order to compare and validate the results for long-term simulations of 25 years (expected lifetime of the system) with a sample time of one hour.

© 2014 Elsevier Ltd. All rights reserved.

1. Introduction

The current situation of the energy sector with a continuous increase in the energy demand, together with the Greenhouse gas emissions and the exhaustion of the fossil fuel reserves have enhanced the combination of renewable energy sources for distributed generation. This combination is denominated Hybrid Renewable Energy Systems (HRES) or simply Hybrid Systems (HS) which are composed by one or more renewable energy sources and energy storage systems (ESS). ESS allow adapting the unregulated power generated by the renewable sources to a specific demanded power. This HS can work in stand-alone [1,2] or grid-connected mode [3–7].

The correct design of the energy dispatching for HS is essential for their operation. energy dispatching strategies are designed to track the load power satisfying secondary objectives such as keeping the charge level of the energy storage devices within their operational limits, minimizing the generation costs, operating the system at high efficiency, reducing the fuel consumption, etc. The papers related to energy dispatching can be classified according to these objectives [8].

Depending on the objectives to meet by the energy dispatching there are two kinds of simulations that can be carried out: short-term and long-term simulations. Short-term simulations are focus on the dynamics of the sources which compose the system and take them into account to face the net power variations due to the changes in load power or disturbances in the renewable energy sources. The length of this kind of simulations goes from 200 s to one day [9–11]. Long-term simulations are used when the main objective is to show the proper operation of the system during a considerable period of time (from months to the whole life of the system) [12–15]. In this case, the dynamics of the energy sources are neglected and they pay attention to other parameters such as operation costs, degradation of the sources, level of charge of the storage devices, etc. Model Predictive Control (MPC) has been widely used in the energy dispatching design because of its ability to deal with constraints in a systematic and straightforward manner. In Ref. [16], the HS was composed by wind turbine, PV, electrolyzer and fuel cell. The energy generated by the renewable sources (both controlled by Maximum Power Point Tracking – MPPT-algorithms) was stored as hydrogen. Depending on if the

* Corresponding author. Tel.: +34 953 648518; fax: +34 953 648586.
E-mail addresses: jtorregl@ujaen.es (J.P. Torreglosa), pablo.garcia@uca.es (P. García), luis.fernandez@uca.es (L.M. Fernández), fjurado@ujaen.es (F. Jurado).

http://dx.doi.org/10.1016/j.renene.2014.08.010
0960-1481/© 2014 Elsevier Ltd. All rights reserved.

دانلود کننده مقالات علمی freepapers.ir FREE papers

Nomenclature

A, B, C	matrices of the HS state space model
A_{bat}	exponential zone amplitude of the battery, (V)
B_{bat}	exponential zone time constant inverse of the battery, $(Ah)^{-1}$
$c_{1,\ldots,6}$	power curve coefficients of the wind turbine, (−)
C_P	power coefficient of the wind turbine, (%)
D_c	duty cycle, (pu)
E_{low,H_2}	lower heating value of hydrogen, (J/kg)
E^0_{bat}	battery constant voltage, (V)
E^{cycle}_{fc}	energy supplied by the fuel cell which reduces the level of the hydrogen tank from 100% to 20%, (Wh)
E^{cycle}_{lz}	energy supplied to the electrolyzer which increases the level of the hydrogen tank from 20% to 100%, (Wh)
E^{char}_{bat}	charge energy that the battery must absorb with the EMS, (Wh)
E^{dis}_{bat}	discharge energy that the battery must deliver with the EMS, (Wh)
E^{year}_{bat}	energy that the battery is expected to deliver during a year, (Wh)
E^{dis}_{fc}	energy that the fuel cell must deliver with the EMS, (Wh)
E^{char}_{lz}	energy that the electrolyzer must absorb with the EMS, (Wh)
E^{char}_{net}	total net charge energy, (Wh)
E^{dis}_{net}	total net discharge energy, (Wh)
ESS	energy storage system
F	Faraday constant, (C/kmol)
H_C	control horizon
H_P	prediction horizon
HRES	hybrid renewable energy systems
I_{ph}	solar-induced current, (A)
I_{ph0}	solar-induced current at a temperature of 300K, (A)
I_{sat}	saturation current of the diode, (A)
i^*	battery filtered current, (A)
i_{bat}	battery current, (A)
$i_{bat}t$	actual battery charge, (Ah)
i_{lz}	electrolyzer current, (A)
K	Boltzmann constant, (JK^{-1})
K_0	constant depending on the characteristics of the PV, (−)
K_1	constant depending on the characteristics of the PV, (−)
K_b	battery polarization constant, (V/(Ah))
k	sampling time
M_{H_2}	total hydrogen mass consumption, (kg)
MPC	model predictive control
MPPT	maximum power point tracking
N	quality factor of the diode of the PV model, (−)
n_{H_2}	produced hydrogen, (mol/s)
n_{lz}	number of electrolyzer cells in series, (−)
P_{fc}	fuel cell power, (W)
P_{load}	power demanded by the load, (W)
P_{lz}	electrolyzer power, (W)
P_{net}	net power, (W)
P_{pv}	power generated by the PV system, (W)
P_{rnw}	power generated by the renewable energy system, (W)
P_{turb}	power captured by the wind turbine blades, (W)
P_{wt}	power generated by the wind turbine, (W)
PEM	proton exchange membrane
PV	photovoltaic
PWM	pulse width modulation
P^{char}_{bat}	battery charge power, (W)
P^{dis}_{bat}	battery discharge power, (W)
p_{H_2}	hydrogen partial pressure, (Pa)
p_{H_2O}	water partial pressure, (Pa)
p_{O_2}	oxygen partial pressure, (Pa)
q	elementary charge of an electron, (C)
Q	battery capacity, (Ah)
q_{H_2in}	hydrogen input flow to the anode, (kg/s)
q_{H_2out}	hydrogen output flow to the anode, (kg/s)
q_{H_2reac}	hydrogen flow that reacts in the anode, (kg/s)
q_{O_2in}	oxygen input flow to the anode, (kg/s)
q_{O_2out}	oxygen output flow to the anode, (kg/s)
q_{O_2reac}	oxygen flow that reacts in the anode, (kg/s)
R_{bat}	battery internal resistance, (Ω)
R_p	PV parallel resistance, (Ω)
R_s	PV series resistance, (Ω)
SOC	state of charge
SPWF	series present worth factor
T_a	aerodynamic torque acting on the blades, (Nm)
T_{pv}	PV operating temperature, (K)
T_{ref}	aerodynamic torque reference, (Nm)
u_{min}	lower constraints for the model inputs
u_{max}	upper constraints for the model inputs
V_{act}	fuel cell activation voltage drop, (V)
V_{bat}	battery voltage, (V)
V_{conc}	fuel cell concentration voltage drop, (V)
V_{fc}	fuel cell output voltage, (V)
V_g	band gap voltage of the semiconductor used in the PV, (V)
V_{irrev}	fuel cell irreversible voltage, (V)
V_{oh}	Fuel cell ohmic voltage drop, (V)
V_{pv}	voltage across the solar cell electrical ports, (V)
v_t	wind speed, (m/s)
W_u	input weight factors
W_y	output weight factors
x, r, u, y	model states, setpoints, manipulated variables and model outputs
y_{min}	lower constraints for the model outputs
y_{max}	upper constraints for the model outputs
η_F	Faraday efficiency, (%)
η_{H_2}	hydrogen system efficiency
η_{bat}	battery efficiency
η_{HS}	HS efficiency
λ	tip speed ratio of the rotor blade tip speed to wind speed, (−)
λ_{O_2}	oxygen excess ratio, (−)
ρ	air density, (kg/m^3)
ω_t	rotational speed, (rad/s)

renewable power was higher or lower than the demanded power, the electrolyzer or the fuel cell worked. Both, the fuel cell and the electrolyzer, had a MPC which generated their reference current subject to their dynamic constrains. The objective of the strategy was to meet the load demand taking into account the dynamic limitations of the energy sources but it was not shown if the strategy is able to maintain the hydrogen level in the tank. Vahidi et al. [17] studied a simple HS for stand-alone applications composed by a fuel cell connected to a load by a DC/DC converter. The fuel cell was assisted by an ultra-capacitor which was directly connected to the DC bus. A MPC generated the reference current of the fuel cell in order to ensure an optimal distribution of current

دانلود کننده مقالات علمی freepapers.ir FREE papers

demand between the two power sources and maintain the oxygen excess ratio of the fuel cell and the ultra-capacitor SOC within their operational limits. The simulations carried out lasted around 20 s and showed that the HS met the control objectives. Kassem et al. [18] presented a system composed by wind turbine and synchronous generator driven by a diesel engine for stand-alone applications. The synchronous generator was directly connected to the three-phase bus and the wind turbine was connected to it by means of an uncontrolled rectifier-inverter (AC-DC-AC). The MPC controlled the diesel motor fuel flow rate and the synchronous generator excitation voltage for regulating the load bus voltage and frequency. The simulations exhibited the ability of the controller to compensate both the wind power oscillations and load disturbances. Another example of MPC for HS was presented in Ref. [19]. In this case, the HS was composed by fuel cell, electrolyzer and wind turbine, and the MPC objective was to generate the water and air flow rates of the fuel cell to keep its temperature and oxygen excess ratio within their safety operation ranges. However, some devices and design, e.g. hydrogen storage, power management and inverters, were not taken into consideration.

It is clear that the use of MPC has been focused in energy dispatching with short-term objectives according to the previous classification. There is a lack of works which propose energy dispatching based on MPC with long-term objectives.

This paper presents a novel energy dispatching based on MPC for an off-grid HS based on wind turbine, PV panels, hydrogen system (composed by FC, electrolyzer and storage tank) and battery. The MPC generates the power to be generated/absorbed by the hydrogen system each hour, taking into account the power limitations of the controlled sources (fuel cell, battery and electrolyzer) and keeping certain levels at the battery SOC and tank hydrogen. The study of the energy dispatching is performed throughout 25 years, which is the estimated life of the HS.

This paper is organized as follows. Section 2 describes the HS under study. The modeling of the components is detailed in Section 3. Section 4 explains the energy dispatching based on MPC applied to the HS, which includes a subsection showing a simple ED used to validate and compare the results obtained with the energy dispatching based on MPC. In Section 5, the simulation results are presented, and finally, the conclusions are established in Section 6.

2. Off-grid HS under study

The HS under study is located in Algeciras (Spain), and it presents the configuration shown in Fig. 1. The new energy dispatching developed in this work is validated for this HS.

In this HS, the main energy sources are the wind turbine and PV panels (renewable sources), whose operation is assisted by the battery and hydrogen system (composed by fuel cell, hydrogen tank and electrolyzer) working as backup and storage systems. In the hydrogen system, the fuel cell is supplied by the hydrogen provided by the tank, which is filled by the electrolyzer. The energy that flows among the energy sources is controlled by DC/DC converters which connect them to a common DC bus. In this HS, when the renewable energy is higher than the energy demanded by the load, this energy excess can be stored as electricity in the battery or as hydrogen in the tank (produced by the electrolyzer). On the other hand, when the renewable energy is lower than the demanded energy, this energy deficit can be supplied by the battery and/or fuel cell.

The sizing of the HS was carried out using Simulink Design Optimization of MATLAB [20], taking as main premise that the fuel cell must be able to provide power for one year without interruption. This premise results in the HS oversizing, which must be taken into account since the excess of generated power involve that the energy dispatching must be designed in order to avoid overcharges in the ESSs.

The sizing method was detailed in Ref. [14] and compared with other sizing methods for a similar HS. The sizing results provide the nominal power of the HS components which fit with the available commercial components summarized in Table 1.

3. Modeling of the system components

This section describes the modeling of the hybrid system components. The models, implemented in SimPowerSystems of MATLAB, were designed from the commercially available components shown in Table 1.

3.1. PV panels

A single-diode model was chosen to represent the behavior of the PV panels. The elements which compose this model are a current source with a diode in parallel which models an ideal PV cell together with a series and a parallel resistance. The use of this model is very common in different works [21,22]. Moreover, it eases finding its parameters in the commercial datasheet [23]. According to this model, the output current of the PV panel is [24]:

$$I_{pv} = I_{ph} - I_{sat}\left(e^{q(V_{pv}+I_{pv}R_s)/(NkT_{pv})}\right) - (V_{pv}+I_{pv}R_s)/R_p \quad (1)$$

$$I_{ph} = I_{ph0}(1 + K_0(T - 300)) \quad (2)$$

$$I_{sat} = K_1 T^3 e^{\left(-\frac{qV_g}{kT}\right)} \quad (3)$$

As shown in Fig. 1, a DC/DC converter connects the PV panels to the DC bus. This converter is controlled by using a MPPT algorithm. The MPPT algorithm is responsible for calculating the PV voltage corresponding to the maximum power point depending on irradiation and temperature conditions. The PV converter controlled by this MPPT algorithm varies the voltage of the PV panels according to the voltage defined by the MPPT algorithm in order to make the PV panels work at any time at the maximum power conditions. The MPPT algorithm consists in a fractional open circuit voltage algorithm which controls the voltage of the PV panels to be proportional to its open-circuit voltage. A PI controller generates the duty cycle of the DC/DC converter from the comparison of the current PV voltage and the open-circuit voltage. The main advantage of this algorithm is its simplicity.

3.2. Wind turbine

The selected wind turbine [25] uses a turbine of two blades with fixed pitch angle and coupled to a three-phase synchronous generator with permanent magnets.

The model of the wind turbine is based on its steady-state power characteristics. The turbine output power is given by the following equation:

$$P_{turb} = \frac{\rho}{2}\pi R^2 v_t^3 C_P(\lambda) \quad (4)$$

The output of this model is the mechanical torque of the wind turbine which depends on the turbine output power and speed:

$$T_a = \frac{P_{turb}}{\omega_t} \quad (5)$$

The electrical power system of this model is composed by a three-phase synchronous generator with permanent magnets, an

freepapers.ir FREE papers

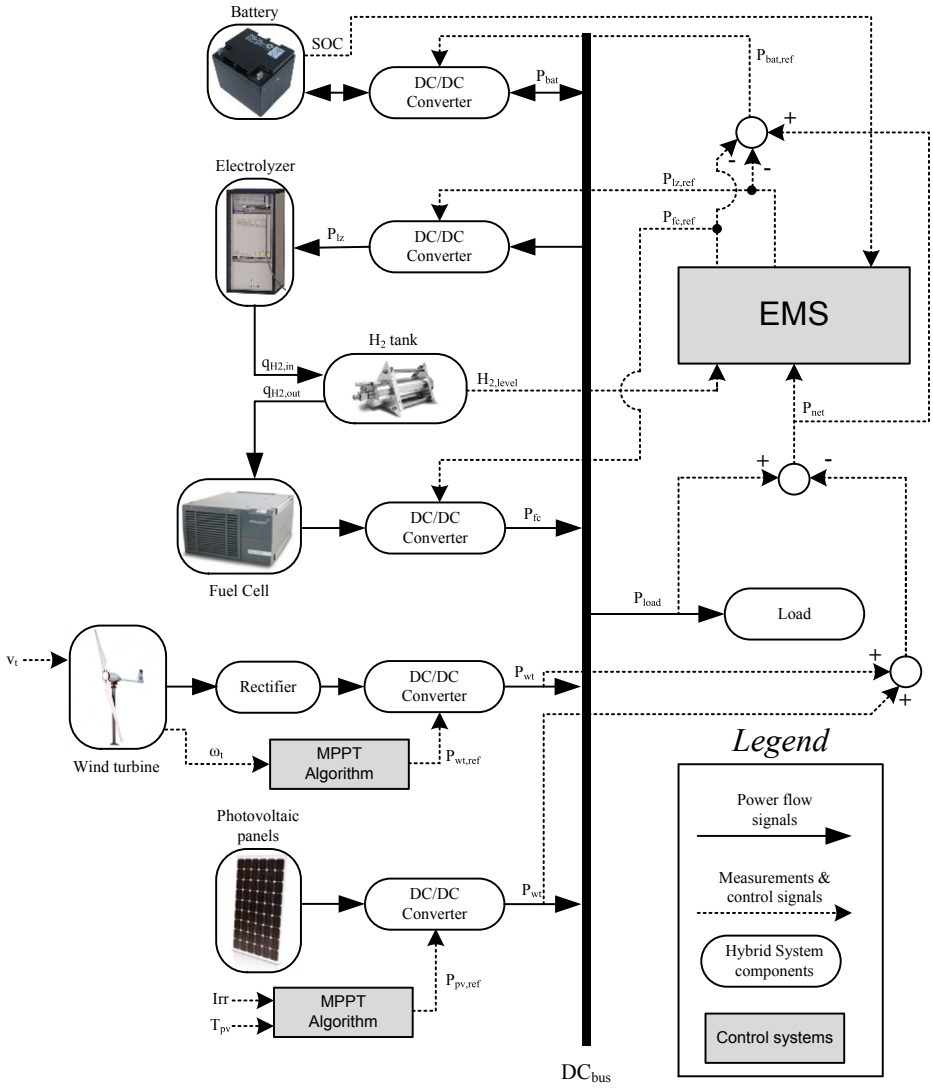

Fig. 1. Off-grid HS under study.

inverter and a DC/DC converter, all of them modeled as average-value equivalent models in SimPowerSystems [26].

Similarly to the PV panels, the wind turbine generation system is connected to the DC bus using a DC/DC converter controlled by a MPPT algorithm based on torque reference. In this case, the MPPT algorithm makes the wind turbine to operate on its maximum C_P for any wind speeds in the below-rated wind speed region by controlling the duty cycle of the DC/DC converter (the variation of the duty cycle produces a variation of its rotational speed). A PI controller compares the reference torque (generated by a look-up table) to the current torque in order to generate the duty cycle of the DC/DC converter.

Table 1
HS components.

Parameter	Value	Component
Photovoltaic array power	1.62 kW	9 × EOPLLY 125M-72 180 W
Wind turbine power	1.50 kW	1 × Bornay 1500
Battery capacity	8.91 kWh	6 × BAE SECURA PVS Solar 660 (in series)
Fuel cell power	1.20 kW	1 × Heliocentris Nexa 1200
Electrolyzer	0.48 kW	1 × Hydrogen Generator HG 60

3.3. Hydrogen system

3.3.1. Fuel cell

Proton Exchange Membrane (PEM) fuel cells, due to its efficiency and good dynamic behavior, meet really well distributed generation demands [14]. The selected model of PEM fuel cell is a simplified version of the model presented in Ref. [27] and whose validity was demonstrated in Ref. [28]. This model has also been widely used to evaluate energy management strategies for hybrid vehicles [29–33]. According to this model, the fuel cell output voltage V_{fc} is given by:

$$V_{fc} = N_{cell} \cdot (E_{cell} - (V_{act} + V_{oh} + V_{conc})) \tag{6}$$

$$E_{cell} = E^0_{cell} - k_e \cdot (T - T_0) - \frac{R \cdot T}{2 \cdot F} \ln\left(\frac{p_{H_2O}}{p^{0.5}_{O_2} \cdot p_{H_2}}\right) \tag{7}$$

Other fuel cell components are the compressor, humidifier, and air cooler. The detailed description of this model can be found in Ref. [28].

freepapers.ir FREE papers

3.3.2. Electrolyzer

The model of the electrolyzer is composed by a resistance. The hydrogen produced by the electrolyzer depends on the current in this resistance and it is calculated using the Faraday's law [34] which is given by

$$n_{H_2} = \frac{\eta_F n_{lz} i_{lz}}{2F} \tag{8}$$

Considering that the electrolyzer temperature is constant, the Faraday efficiency is the following [34]:

$$n_F = 96.5e^{\left(0.09/i_{lz} - 75.5/i_{lz}^2\right)} \tag{9}$$

Combining Eqs. (8) and (9) leads to a simple model of the electrolyzer.

3.4. Battery

The use of batteries as energy storage devices for off-grid power supplies is widely extended [35,36]. Lead-acid batteries present a good performance for this kind of applications and its low price in comparison to the rest of battery technologies [37] was determinant for selecting them for this work. The battery model was taken from the SimPowerSystems toolbox of Simulink which corresponds to the model presented in Ref. [38]. This model is composed by a variable voltage source and a series resistor. The variable voltage is calculated using the following expression:

$$V_{bat} = E^0_{bat} - K_b \cdot \frac{Q}{Q - i_{bat}t} i_{bat} t - R_{bat} i_{bat} + A_{bat} \exp(-B_{bat} \cdot i_{bat} t) - K_b \cdot \frac{Q}{Q - i_{bat}t} i^*_{bat} \tag{10}$$

3.5. DC/DC converters

Finally, different PWM-based DC/DC converters [39], summarized in Table 2, are used to connect the different energy sources to the DC bus. These converters allow controlling the energy flow between the sources adapting their variable voltages to the constant DC bus voltage.

Average-value equivalent models (composed by current and voltage sources) represent these converters in this work. This kind of model reproduces the dynamic of the converters for large sample times.

4. Energy dispatching

4.1. Energy dispatching based on MPC

The energy dispatching based on a MPC scheme generates the power of the hydrogen system (P_{H_2}), which can be positive or negative depending on if it is the fuel cell or the electrolyzer which operates. Fig. 2 shows the overall scheme of the proposed control strategy. As can be seen, a subsystem calculates the reference powers for the fuel cell, electrolyzer and battery from the P_{H_2} generated by the MPC and the net power. This net power is defined as:

$$P_{net} = P_{load} - P_{pv} - P_{wt} \tag{11}$$

where P_{load} is the power demanded by the load, P_{pv} is the power generated by the PV panels and P_{wt} is the power generated by the wind turbine.

According to the expression (12), if the sum of P_{pv} and P_{wt} is higher than P_{load}, there is an energy surplus that must be stored as electricity in the battery or as hydrogen generated by the electrolyzer. On the other hand, if the sum of P_{pv} and P_{wt} is lower than P_{load}, the system needs to discharge the battery or activate the fuel cell to meet the power demand.

With regard to the MPC, a linear time-invariant model of the off-grid HS under study is required as the first step for designing the predictive controller. The state-space model of the system was obtained using the Simulink Control Design Toolbox. It allows to linearize continuous-time, discrete-time (which is the case of this work), or multirate Simulink models. The linearization point of the model corresponds to a steady-state operating point of the model which occurs when the system is in equilibrium or trim condition which means that state variables that do not change with time. The resulting time-invariant model is in state-space form. Simulink Control Design uses a block-by-block approach to linearize the models which individually linearizes each block of the whole model and combines the results to produce the linearization of the specified system. This model has one input, the power of the hydrogen system (P_{H_2}), which is generated by the predictive controller. The model outputs are: 1) the power generated by the controllable power sources (P_{gen}), which is the sum of the powers of the battery, the fuel cell and the electrolyzer; 2) the battery SOC (SOC); and 3) the hydrogen level ($H_{2,level}$). This linear model is obtained by using the Control Design Toolbox® of MATLAB. The off-grid system can be represented by a state space model which has the following form:

$$\begin{cases} x(k+1) = Ax(k) + Bu(k) \\ y(k) = Cx(k) \end{cases} \tag{12}$$

where k is the sampling time, A, B, and C are matrices of appropriate dimensions, and x, u, and y are the model states, manipulated variables, and model outputs, respectively. After linearizing and discretizing, the following space model is obtained:

$$\begin{cases} y = \begin{bmatrix} P_{gen} & SOC & H_{2,level} \end{bmatrix}^T \\ u = \begin{bmatrix} P_{H_2} \end{bmatrix} \\ A = \begin{bmatrix} 3.359e^{-31} & 2.29e^{-34} & 4.503e^{-30} \\ -1 & 0.03567 & 4.901e^{-5} \\ -0.07455 & 4.904e^{-5} & 1 \end{bmatrix} \\ B = \begin{bmatrix} -1 & 2.29e^{-34} & 4.503e^{-30} \end{bmatrix}^T \\ C = \begin{bmatrix} -1 & -0.9643 & 4.901e^{-5} \\ -6.827e^{-31} & 7.706e^{-6} & -0.1515 \\ -1.407e^{-27} & -0.01588 & 0.213 \end{bmatrix} \end{cases} \tag{13}$$

Once the model is defined, the controller is designed. The main objective of the predictive controller is to hold the outputs y at the reference values (or setpoints) r by adjusting the manipulated variables (or actuators) u. The predictive controller generates the manipulated variables predicting the future behavior of the system using the off-grid HS model mentioned in Section 3 and shown in Fig. 2.

Table 2
Summary of the HS DC/DC converters.

Power source	Converter	Energy flow (From → To)
PV	Unidirectional – Boost	(PV → DC bus)
WT	Unidirectional – Buck	(WT → DC bus)
Battery	Bidirectional	(Battery → DC bus) – Boost (DC bus → Battery) – Buck
FC	Unidirectional – Boost	(FC → DC bus)
Electrolyzer	Unidirectional – Boost	(DC bus → Electrolyzer)

freepapers.ir FREE papers

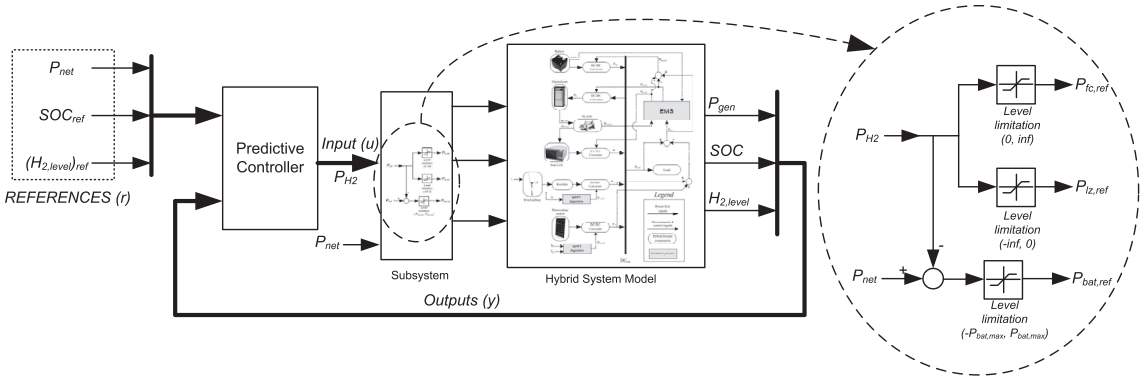

Fig. 2. Overall scheme of the energy dispatching based on MPC.

The model predictive controller is designed to minimize the following finite horizon control and performance index:

$$\min_{u} \quad J(x(t),u(t),t) = \begin{cases} \sum_{k=1}^{H_P} W_y \left[y(k) - y(k)_{\text{ref}} \right]^2 \\ + \sum_{k=1}^{H_C} W_u \left[u(k) - u(k)_{\text{ref}} \right]^2 \end{cases} \tag{14}$$

$$\text{subject} \quad \text{to}: \begin{cases} y(k)_{\min} < y(k) < y(k)_{\max} \\ u(k)_{\min} < u(k) < u(k)_{\max} \end{cases} \tag{15}$$

where W_y and W_u are the input and output weight factors for each variable, and H_P and H_C are the prediction and control horizons, respectively.

The objective function is subjected to a set of constraints, consisting of the input and output upper and lower limits, which are summarized in Table 3. The output power upper and lower limits ($y_{\max}$, $y_{\min}$) are defined by the maximum operating powers of the fuel cell and electrolyzer.

The controller ensures that the two requirements are met: 1) track the load power; and 2) keep the battery SOC and hydrogen tank level between their reference values.

The MPC is completed with two auxiliary switches which disconnect the renewable power sources (PV and wind turbine) when the battery SOC is higher than 95%.

The MPPT controls of the PV and wind turbine are considered independent of the energy dispatching.

To validate the energy dispatching proposed in this work, a simpler energy dispatching based on state control is presented in the next subsection.

Table 3
Summary of the controller parameters.

Controller parameters		
Control interval (h)	1	
Prediction horizon (intervals)	3	
Control horizon (intervals)	2	
Output constrains	**Type**	**Range**
Load power generated (kW)	Level limitation	[-3000,1800]
Battery SOC (%)	Level limitation	[20,95]
SC SOC (%)	Level limitation	[20,95]
Input constrains	**Type**	**Range**
Hydrogen power (W)	Level limitation	[-480,1200]
Reference values		
Load power generated (kW)		P_{net}
Battery SOC (%)		60
SC SOC (%)		60

4.2. Energy dispatching based on state control

This energy dispatching uses a simple state-machine control to determinate the power of the battery, fuel cell and electrolyzer depending on the net power, battery SOC and hydrogen level. The flowchart presented in Fig. 3 shows the different operation states.

Three levels of battery SOC and hydrogen in the tank have been considered (high, H; normal, N; and low, L). The changes among these levels are performed by using the hysteresis cycles shown Fig. 3.

Both energy dispatching have switches to disconnect the renewable power sources and to avoid overcharges of the storage units.

5. Simulation results

The control strategies presented in this work were simulated for 25 years (the estimated lifetime of the HS) with a sample time of one hour to evaluate and validate the performance of the proposed energy dispatching based on MPC. The sample time of one hour was chosen since it is short enough taking into account that the objective of the paper is to check the performance of the strategies along the whole lifetime of the system (25 years). The HS model and control strategies were simulated in Simulink-MATLAB by using its discrete solver.

Fig. 4 shows the sun irradiance, wind speed and load power consumption profile used in the simulations. The solar irradiance and wind speed data were collected hourly from a weather station located in Algeciras (Spain) during a year. The load power consumption profiles were collected hourly during four different days corresponding to different seasons (as shown Fig. 5). Each one represented the typical power demand for each season and was extrapolated over the period of time corresponding to that season. Finally, they were extrapolated over the lifetime of the HS.

Figs. 6 and 7 show the power of the controlled power sources, battery and fuel cell/electrolyzer system, for both energy dispatchings, during one year of operation (specifically the first year of operation). It can be observed that the hydrogen power variation is lower for the energy dispatching based on MPC, and therefore, its battery power range is higher. Furthermore, the resulting hydrogen power profile is more symmetrical which means that the fuel cell and the electrolyzer operate under similar power requirements, far from their maximum power limits. This fact represents an advantage since the fuel cell efficiency is higher for low power demands. In the case of the energy dispatching based on states, the hydrogen power varies in a higher range: the electrolyzer is off during more time, its maximum power is reached frequently, and the fuel cell operates at higher powers

freepapers.ir FREE papers

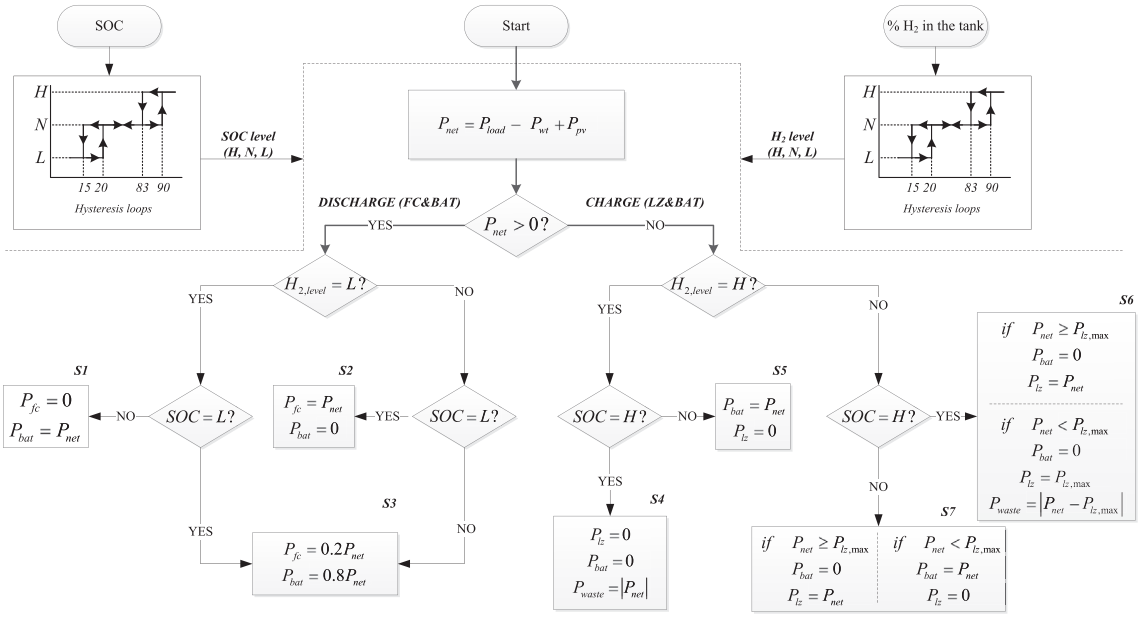

Fig. 3. Flowchart of the energy dispatching based on state control.

which means working at lower efficiencies compared to the case of the MPC energy dispatching. With regard to the battery power, represented for the first year of operation in Fig. 7, it is shown that the magnitude of the battery discharge power is higher for the MPC energy dispatching which produces a higher variation in its SOC (it reaches a lower value) and leads to a more frequent operation of the battery in the charging mode. Therefore, the battery operation time is higher for the energy dispatching based on MPC than for the one based on states.

The battery SOC and the hydrogen tank level are depicted in Fig. 8 for the whole life of the HS. Due to the fact that the battery and hydrogen system power variations are higher for the energy dispatching based on MPC, its variation range of SOC and hydrogen tank level is wider (around a 40% for the SOC and a 60% for the hydrogen tank level versus a 25% for both in the energy dispatching based on states – neglecting occasional peaks). Apart from that, it can be noticed that, for both strategies, the variations in the battery SOC and hydrogen level increase as the time progresses (although it is more noticeable for the energy dispatching based on states). These variations across the time are almost negligible for the battery SOC, but they are notable for the hydrogen tank level. With regard to the variation range, it is shown that, for both strategies,

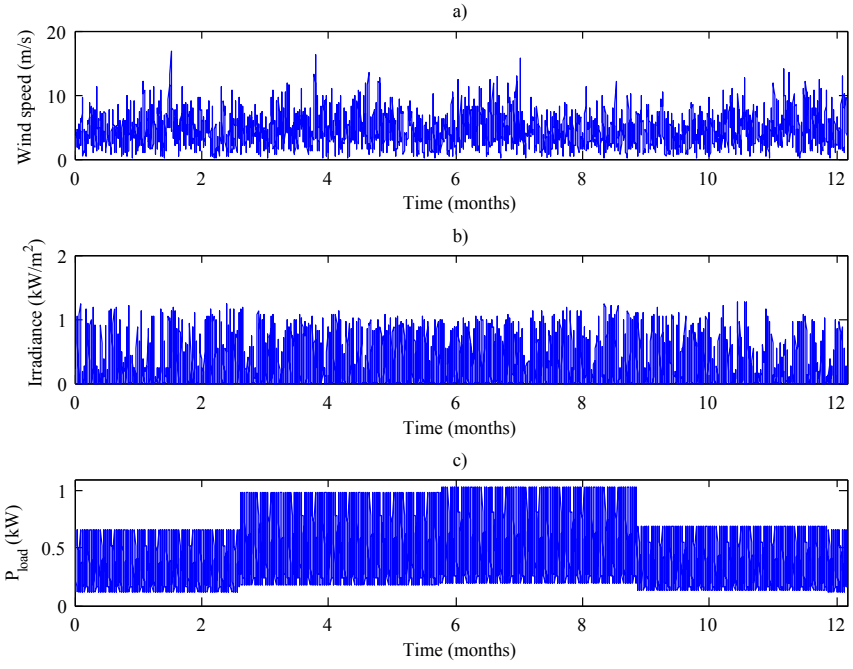

Fig. 4. Collected data for one year: a) Solar irradiance, b) Wind speed, and c) Load power profile.

freepapers.ir FREE papers

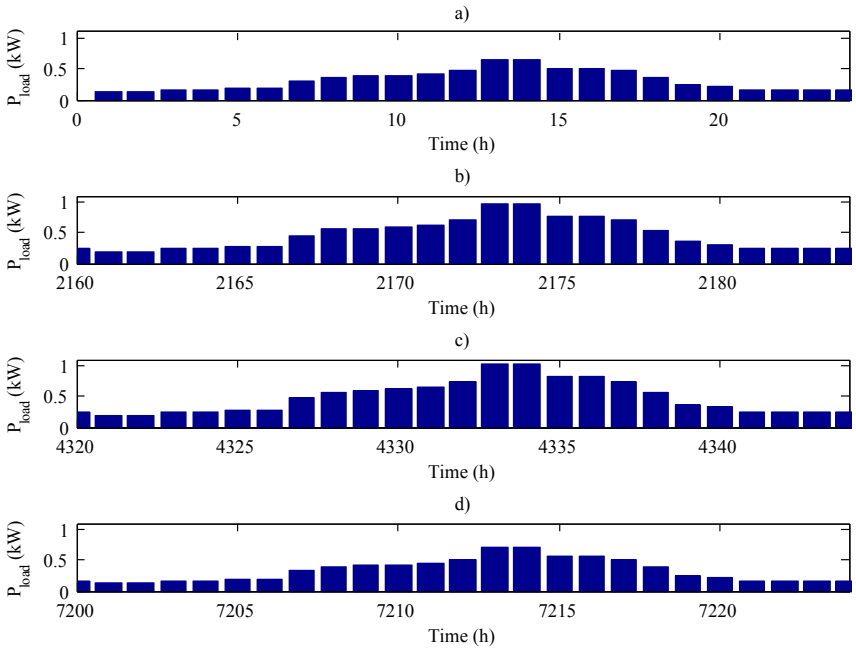

Fig. 5. Daily load power consumption profiles.

the hydrogen level varies much more than the battery SOC, reaching low hydrogen levels. The battery average SOC is kept around 74% for the energy dispatching based on MPC and around 85% for the energy dispatching based on state control, with higher variation ranges for the first one. The hydrogen average level of the tank is higher for the energy dispatching based on states, approximately 81%, whereas, for the MPC based energy dispatching, it is around 53%.

Finally, Fig. 9 shows the efficiency of the HS, hydrogen system and battery which are calculated from Eqs. 16–18 [14]. The resulting HS efficiency for the strategy based on MPC is 69.45%, which is noticeably higher than the resulting of 54.8% for the strategy based on states, and thus, achieving a more efficient management of the energy sources of HS.

Focusing on the backup and storage systems, the hydrogen system efficiencies are quite similar (31.98%), and the MPC strategy presents better battery efficiency compared with the states strategy (72.61% versus 60.38%). This improvement in the battery efficiency is a consequence of the symmetry of the battery power profile in the MPC strategy which means that the upper and lower

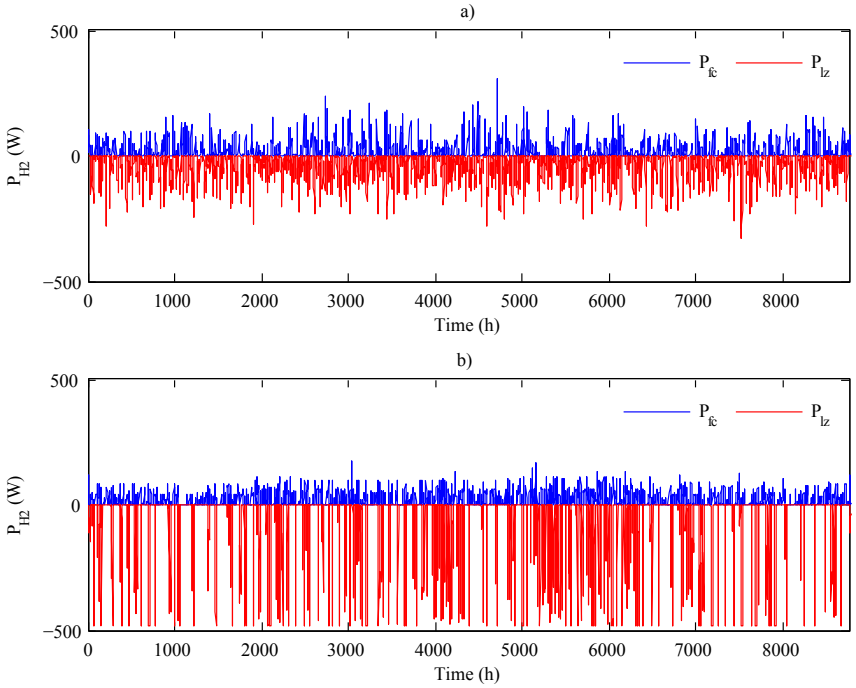

Fig. 6. FC and electrolyzer powers for: a) Energy dispatching based on MPC, and b) Energy dispatching based on state control.

freepapers.ir FREE papers

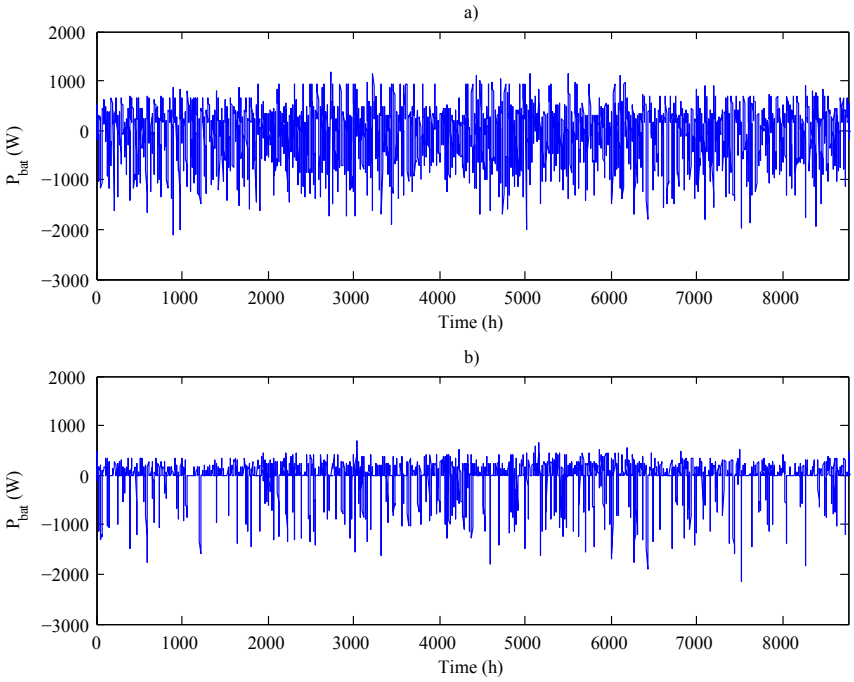

Fig. 7. Battery power for: a) Energy dispatching based on MPC, and b) Energy dispatching based on state control.

terms of Eq. (18) are closer and the fraction is nearer to 1 than in the states strategy in which the lower term is higher (due mainly to the difference in magnitude between discharge and charge powers). In the case of the hydrogen system efficiency, although at first glance it would seem that the MPC strategy should have better efficiency due to a higher symmetry of the hydrogen system power profile, in the states control the charge power magnitude is higher than the discharge but its lower operation time compensates this difference leading to an efficiency similar to the other energy dispatching.

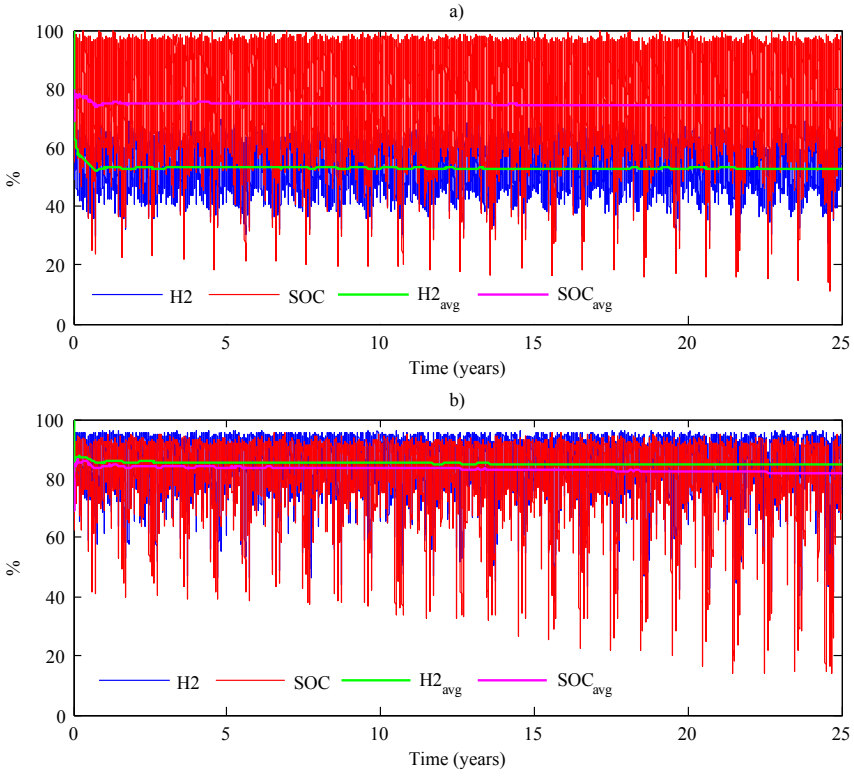

Fig. 8. Battery SOC and hydrogen tank level for: a) Energy dispatching based on MPC, and b) Energy dispatching based on state control.

freepapers.ir FREE papers

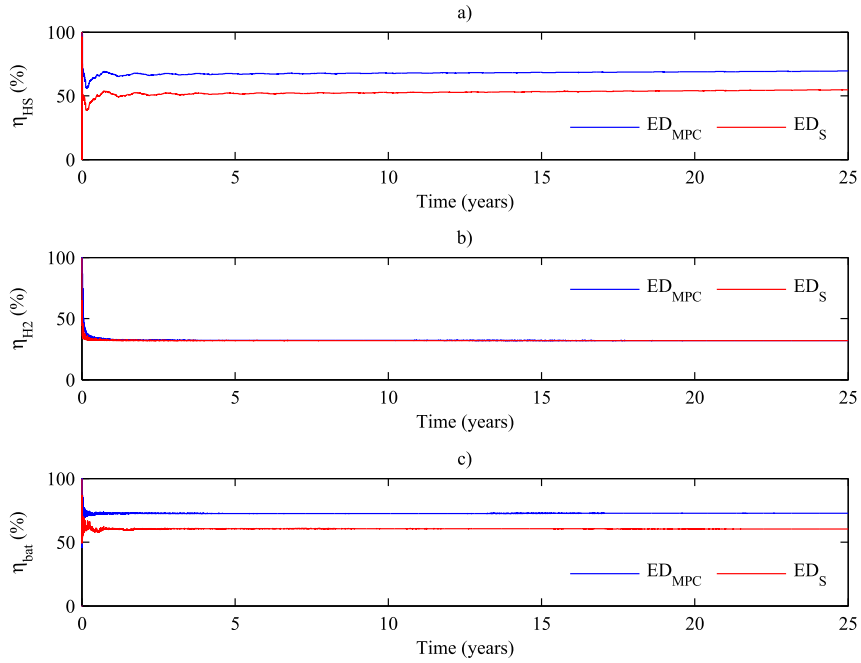

Fig. 9. Efficiency of the: a) HS; b) hydrogen system; c) battery.

$$\eta_{HS} = \frac{\int_{cycle} P_{load}\,dt}{\int_{cycle} P_{rnw}\,dt + E_{low,H_2}\int_{cycle} M_{H_2}\,dt + \int_{cycle} P_{bat}\,dt} \times 100 \tag{16}$$

$$\eta_{H_2} = \frac{\eta_{lz,con}\,\eta_{fc,con}\int_{cycle} P_{fc}\,dt}{\int_{cycle} P_{lz}\,dt} \times 100 \tag{17}$$

$$\eta_{bat} = \frac{\eta^2_{bat,con}\int_{cycle} P^{dis}_{bat}\,dt}{\int_{cycle} P^{char}_{bat}\,dt} \times 100 \tag{18}$$

where P_{load} is the power supplied to the load, P_{rnw} is the power supplied by the renewable sources, E_{low,H_2} is the lower heating value of hydrogen, and $\eta_{lz,con}$, $\eta_{fc,con}$, $\eta_{bat,conv}$ are the efficiencies of the DC/DC converters corresponding to each source.

6. Conclusions

The main contribution of this work has been to present and evaluate an energy dispatching based on MPC for an off-grid HS integrating wind turbine, PV panels, hydrogen system and battery. In this HS, the renewable energy sources generate the maximum available power, whereas the energy dispatching is responsible for controlling the operation of battery and hydrogen system.

In this energy dispatching, the predictive controller determines the power of the hydrogen system (positive for the fuel cell and negative for the electrolyzer) taking into account the power generated by the controllable power sources, the battery SOC, and the hydrogen level. The battery power is obtained from the difference between the net power (load power minus PV power and wind turbine power) and the hydrogen system.

The energy dispatching based on MPC was validated by comparison with an ED based on state control. The simulation results, obtained for the estimated lifetime of the HS (25 years), demonstrated that the energy dispatching based on MPC achieved a higher global efficiency of the HS, assuring the off-grid load support and keeping the battery SOC and hydrogen level between the desired operating limits.

Acknowledgments

This work was supported by the Spanish Ministry of Science and Innovation under Grant ENE2010-19744/ALT.

References

[1] Gupta Ajai, Saini RP, Sharma MP. Modelling of hybrid energy system—Part II: combined dispatch strategies and solution algorithm. Renew Energy 2011;36(2):466–73.
[2] Lujano-Rojas JM, Monteiro C, Dufo-López R, Bernal-Agustín JL. Optimum load management strategy for wind/diesel/battery hybrid power systems. Renew Energy 2012;44:288–95.
[3] Lagorse J, Paire D, Miraoui A. A multi-agent system for energy management of distributed power sources. Renew Energy 2010;35(1):174–82.
[4] Ghoddami H, Delghavi MB, Yazdani A. An integrated wind-photovoltaic-battery system with reduced power-electronic interface and fast control for grid-tied and off-grid applications. Renew Energy 2012;45:128–37.
[5] Paiva JE, Carvalho AS. Controllable hybrid power system based on renewable energy sources for modern electrical grids. Renew Energy 2013;53:271–9.
[6] Azcárate C, Blanco R, Mallor F, Garde R, Aguado M. Peaking strategies for the management of wind-H_2 energy systems. Renew Energy 2012;47:103–11.
[7] Tofighi A, Kalantar M. Power management of PV/battery hybrid power source via passivity-based control. Renew Energy 2011;36(9):2440–50.
[8] Torreglosa JP, García P, Fernández LM, Jurado F. Hierarchical energy management system for stand-alone hybrid system based on generation costs and cascade control. Energy Convers Manag 2014;77:514–26.
[9] Wang C, Nehrir MH. Power management of a stand-alone wind/photovoltaic/fuel cell energy system. IEEE Trans Energy Convers 2008;23(3):957–67.

[10] Thounthong P, Chunkag V, Sethakul P, Sikkabut S, Pierfederici S, Davat B. Energy management of fuel cell/solar cell/supercapacitor hybrid power source. J Power Sources 2011;196(1):313–24.
[11] Onar OC, Uzunoglu M, Alam MS. Modeling, control and simulation of an autonomous wind turbine/photovoltaic/fuel cell/ultra-capacitor hybrid power system. J Power Sources 2008;185(2):1273–83.
[12] Dufo-López R, Bernal-Agustín JL, Contreras J. Optimization of control strategies for stand-alone renewable energy systems with hydrogen storage. Renew Energy 2007;32(7):1102–26.
[13] Dufo-López R, Bernal-Agustín JL. Design and control strategies of PV-diesel systems using genetic algorithms. Sol Energy 2005;79(1):33–46.
[14] Castañeda M, Cano A, Jurado F, Sánchez H, Fernández LM. Sizing optimization, dynamic modeling and energy management strategies of a stand-alone PV/hydrogen/battery-based hybrid system. Int J Hydrogen Energy 2013;38(10):3830–45.
[15] Ipsakis D, Voutetakis S, Seferlis P, Stergiopoulos F, Elmasides C. Power management strategies for a stand-alone power system using renewable energy sources and hydrogen storage. Int J Hydrogen Energy 2009;34(16):7081–95.
[16] Trifkovic M, Sheikhzadeh M, Nigim K, Daoutidis P. Modeling and control of a renewable hybrid Energy system with hydrogen storage. IEEE Trans Control Syst Technol 2014;22(1):169–79.
[17] Vahidi A, Stefanopoulou A, Peng Huei. Current management in a hybrid fuel cell power system: a model-predictive control approach. IEEE Trans Control Syst Technol 2006;14(6):1047–57.
[18] Kassem AM, Yousef AM. Voltage and frequency control of an autonomous hybrid generation system based on linear model predictive control. Sustain Energy Technol Assessments 2013;4:52–61.
[19] Wu W, Xu JP, Hwang JJ. Multi-loop nonlinear predictive control scheme for a simplistic hybrid energy system. Int J Hydrogen Energy 2009;34(9):3953–64.
[20] MathWorks Inc.. Simulink design optimization. Natick, MA; 2010.
[21] Kim W, Duong V-H, Nguyen T-T, Choi W. Analysis of the effects of inverter ripple current on a photovoltaic power system by using an AC impedance model of the solar cell. Renew Energy 2013;59:150–7.
[22] Li S, Haskew TA, Li D, Hu F. Integrating photovoltaic and power converter characteristics for energy extraction study of solar PV systems. Renew Energy 2011;36(12):3238–45.
[23] Eoplly New Energy Technology Co, Ltd. EOPLLY 125MF/72(185-200W) datasheet. [Online], http://www.eoplly.com/Htdocs/manager/upfile/upfile/20131126576724 21.pdf.
[24] Gow JA, Manning CD. Development of a photovoltaic array model for use in power-electronics simulation studies. IEE Proc Electr Power Appl 1999;146(2):193–200.
[25] Bornay Aerogeneradores, slu. Bornay 1500 Datasheet. [Online], available: http://www.bornay.com/eolica/en/wind-turbines/4/models/17/bornay-1500/2.
[26] The MathWorks, Inc. SimPowerSystems. [Online], http://www.mathworks.es/products/simpower/.
[27] Pukrushpan JT, Stefanopoulou AG, Peng H. Control of fuel cell power systems: principles, modeling, analysis, and feedback design. London: Springer Verlag; 2002.
[28] Garcia P, Fernández LM, Garcia CA, Jurado F. Comparative study of PEM fuel cell models for integration in propulsion systems of urban public transport. Fuel Cells 2010;10(6):1024–39.
[29] García P, Fernández LM, Garcia CA, Jurado F. Energy management system of fuel cell-battery hybrid tramway. IEEE Trans Ind Electron 2009;57(12):4013–23.
[30] Fernandez LM, Garcia P, Garcia CA, Torreglosa JP, Jurado F. Comparison of control schemes for a fuel cell hybrid tramway integrating two dc/dc converters. Int J Hydrogen Energy 2010;35(11):5731–44.
[31] García P, Torreglosa JP, Fernández LM, Jurado F. Viability study of a FC-battery-SC tramway controlled by equivalent consumption minimization strategy. Int J Hydrogen Energy 2012;37(11):9368–82.
[32] Torreglosa JP, Garcia P, Fernandez L, Jurado F. Predictive control for the Energy management of a fuel cell-battery-supercapacitor tramway. IEEE Trans Ind Inform 2014;10(1):276–85.
[33] García P, Torreglosa JP, Fernández LM, Jurado F. Control strategies for high-power electric vehicles powered by hydrogen fuel cell, battery and supercapacitor. Expert Syst Appl 2013;40(12):4791–804.
[34] Uzunoglu M, Onar OC, Alam MS. Modeling, control and simulation of a PV/FC/UC based hybrid power generation system for stand-alone applications. Renew Energy 2009;34(3):509–20.
[35] Dalton GJ, Lockington DA, Baldock TE. Feasibility analysis of stand-alone renewable energy supply options for a large hotel. Renew Energy 2008;33(7):1475–90.
[36] Fux SF, Benz MJ, Guzzella L. Economic and environmental aspects of the component sizing for a stand-alone building energy system: a case study. Renew Energy 2013;55:438–47.
[37] Linden D, Reddy TB. Handbook of batteries. New York: McGraw- Hill; 2002.
[38] Tremblay O, Dessaint LA. Experimental validation of a battery dynamic model. EV Appl World Electr Veh J 2009;3(1).
[39] Kazimierczuk MK. Pulse-width modulated DC-DC power converters. s.l.: Willey; 2008.

freepapers.ir FREE papers